Double compression-expansion engine (DCEE) fueled with hydrogen: Preliminary computational assessment

Transportation Engineering 8 (2022) 100103

Contents lists available at ScienceDirect

Transportation Engineering

journal homepage: www.sciencedirect.com/journal/transportation-engineering

Full Length Article

Double compression-expansion engine (DCEE) fueled with hydrogen: Preliminary computational assessment

Rafig Babayev [a,*], Arne Andersson [b], Albert Serra Dalmau [b], Hong G. Im [c], Bengt Johansson [a]

[a] Combustion Engine Research Center (CERC), Chalmers University of Technology, Sweden
[b] Powertrain Strategic Development (PSD), Volvo Group Trucks Technology (Volvo GTT), Sweden
[c] Clean Combustion Research Center (CCRC), King Abdullah University of Science and Technology (KAUST), Saudi Arabia

ARTICLE INFO

Keywords:
Hydrogen
Combustion engine
Compression ignition
Double compression-expansion engine (DCEE)
CFD
Optimization

ABSTRACT

Hydrogen (H_2) is currently a highly attractive fuel for internal combustion engines (ICEs) owing to the prospects of potentially near-zero emissions. However, the production emissions and cost of H_2 fuel necessitate substantial improvements in ICE thermal efficiency. This work aims to investigate a potential implementation of H_2 combustion in a highly efficient double compression-expansion engine (DCEE). DICI nonpremixed H_2 combustion mode is used for its superior characteristics, as concluded in previous studies. The analysis is performed using a 1D GT-Power software package, where different variants of the DICI H_2 and diesel combustion cycles, obtained experimentally and numerically (3D CFD) are imposed in the combustion cylinder of the DCEE. The results show that the low jet momentum, free jet mixing dominated variants of the DICI H_2 combustion concept are preferred, owing to the lower heat transfer losses and relaxed requirements on the fuel injection system. Insulation of the expander and removal of the intercooling improve the engine efficiency by 1.3 and 0.5%-points, respectively, but the latter leads to elevated temperatures in the high-pressure tank, which makes the selection of its materials harder but allows the use of cheaper oxidation catalysts. The results also show that the DCEE performance is insensitive to combustion cylinder temperatures, making it potentially suitable for other high-octane fuels, such as methane, methanol, ammonia, etc. Finally, a brake thermal efficiency of 56% is achieved with H_2 combustion, around 1%-point higher than with diesel. Further efficiency improvements are also possible with a fully optimized H_2 combustion system.

Definitions/Abbreviations

aTDC	after top dead center
BTE	brake thermal efficiency
CAC	charge air cooler
CAD	crank angle degree
CDC	conventional diesel combustion
CFD	computational fluid dynamics
CI	compression ignition
DCEE	double compression-expansion engine
DI	direct injection
EGR	exhaust gas recirculation
EVO	exhaust valve opening
FMEP	friction mean effective pressure
FuelMEP	fuel mean effective pressure
GIE	gross indicated efficiency
HP	high-pressure
HT	heat transfer
HTM	heat transfer multiplier
ICE	internal combustion engine
IMEP	indicated mean effective pressure
$IMEP_{gross}$	gross indicated mean effective pressure
IVC	inlet valve closing
LP	low-pressure
PCP	peak cylinder pressure (after combustion)
PMP	peak motoring pressure
RPM	revolutions per minute
SCR	selective catalytic reduction
SI	spark ignition
TDC	top dead center
γ	specific heat ratio
λ	air-fuel equivalence ratio

* Corresponding author.
E-mail address: rafik.babayev01@gmail.com (R. Babayev).

https://doi.org/10.1016/j.treng.2022.100103
Received 20 May 2021; Received in revised form 19 July 2021; Accepted 7 January 2022
Available online 10 January 2022

1. Introduction

Hydrogen (H_2) internal combustion engines (ICEs) are now a subject of intense research owing to rising interest and vast investments into H_2 technologies for their potentially low carbon footprint. Energy conversion efficiency also became increasingly more important consideration in the development of modern ICEs. With conventional hydrocarbon fuels, the most obvious path to lower tail-pipe CO_2 emissions is through improvements in energy conversion efficiency. Hydrogen engines, on the other hand, can produce negligibly small amounts of tail-pipe CO_2, with only trace amounts from lubricant oil, which may potentially be eliminated. Thus, the CO_2 emissions and cost associated with H_2 fuel *production* are more crucial considerations. In 2020, 95% of H_2 production in the U.S. was sourced from natural gas via steam methane reforming (SMR) process, while globally SMR accounts for 76% of H_2 production [1]. Currently, the carbon footprint of H_2 production via SMR is estimated to be in the range of 40 gCO_2/MJ [2] at 1.43 – 2.27 $/kg (0.012 – 0.019 $/MJ) with CO_2 capture and storage. However, H_2 fuel distribution and storage, combined with the relatively low production and utilization volumes, incur substantially higher costs for consumers. For example, according to [3], the average price of H_2 for fuel cell vehicles in California was 16.51 $/kg in 2019, which is around 18 $ per equivalent (in terms of energy content) gallon of diesel. Thus, to further reduce the well-to-wheels emissions and cost of operation of vehicles powered by H_2 ICEs, continued improvement of engine efficiency is of utmost importance. This is especially critical for commercial transport sector, which is more cost-sensitive and where H_2 engines are expected to be the most prevalent.

A relatively new split-cycle engine concept, the double compression-expansion engine (DCEE) [4–7] promises significant improvements in energy conversion efficiency at low cost. The principal layout of the system is given in Fig. 1. The base version consists of three dedicated cylinders: compressor, combustor, and expander units. The compressor and expander units are fed from two accumulator tanks, one at low pressures (LP) with a charge air cooler (CAC), and the other – at high pressures (HP). The compressor and expander cylinders, which are two-stroke mechanisms, operate at relatively low pressures, while the combustor cylinder, a four-stroke mechanism, operates at high pressures. The combustor unit is essentially a combustion cylinder of a conventional compression-ignition (CI) engine with minor modifications (primarily reduced compression ratio). The operating principle of the DCEE includes two-stage compression process, first in the compressor, then in the combustor units, and two-stage expansion process, first in the combustor, then in the expander units. Splitting the thermodynamic cycle between the three dedicated units offers greater flexibility for optimization of engine performance, efficiency, and emissions characteristics. For example, the size of the combustor unit can be minimized to reduce heat transfer and friction losses. The expander unit, on the other hand, can have larger displacement and higher expansion ratio compared to the compressor. This enables the expander to extract work more efficiently from the large amount of exhaust gasses at relatively low pressures and temperatures, and achieve overexpanded cycle, with additional benefits from improved mechanical efficiency. The dedicated compressor and expander cylinders may also be more easily insulated, thus further reducing heat transfer losses. This is also the case for LP and HP tanks. More effective emissions aftertreatment may also be incorporated into the HP tank owing to its consistently higher temperatures than those of the exhaust of regular engines. The expander cylinder may also be used for ammonia injections, or an H_2-SCR may be installed downstream of the expander for effective aftertreatment. This will be discussed in more detail in Section 2.1. Multiple computational and experimental studies showed that the DCEE is capable of achieving around 53–55% brake thermal efficiency (BTE) with conventional diesel combustion (CDC).

Owing to the high efficiency and flexibility of the DCEE concept, it is suitable for use with H_2 fuel. The high thermal efficiency of this engine is achieved not only via reduced heat transfer losses, but also via the high effective compression ratio (compressor + combustor) leading to high peak cylinder pressures, up to 300 bar. Thus, premixed spark-ignition (SI) mode of combustion is not ideal for realizing the full potential of the engine concept, due to the knock and other limitations [8]. Instead, a direct-injection compression-ignition (DICI) H_2 combustion mode (like in diesel engines) is implemented in the combustor unit of the DCEE.

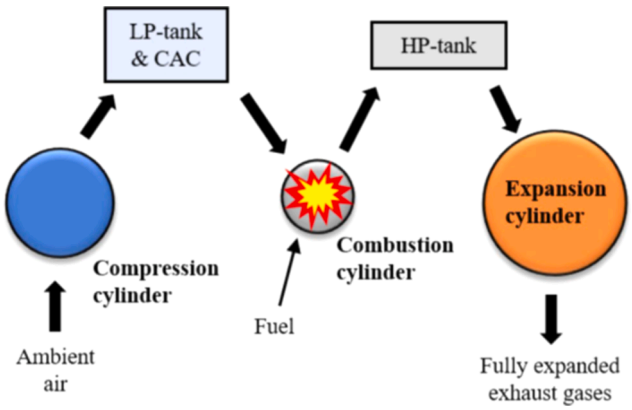

Fig. 1. Principal layout of the double compression-expansion engine (DCEE) [6].

The DICI H_2 combustion concept was thoroughly investigated in our previous studies using computational fluid dynamics (CFD). It was first characterized in [9], then compared to an equivalent diesel fuel combustion [8], and the findings were used to develop a new optimization path specifically suited for DICI H_2 engines [10]. It was found that, unlike with conventional diesel engines, combustion governed by free turbulent jet mixing is more suitable for DICI H_2 engines than the drastically more common momentum-dominated global mixing. This is due to the faster burning rate and, simultaneously, lower heat transfer losses in the former mixing mode, achieved by utilizing unique characteristics of H_2 fuel (gaseous state, low density, high injection velocity, and flow structures [8]) and by minimizing jet momentum, hence, flame-wall contact [10]. Thus, the free jet mixing was promoted in [10], leading to substantial improvements in engine indicated efficiency. The details of the implemented modifications are given in Section 2. As a result, 5 generations of the DICI H_2 combustion system were obtained.

The present work computationally incorporates the most promising variants of the DICI H_2 combustion concept (4 generations out of total 5) into the DCEE system using a 1D model developed in the GT-Power engine simulation software [11]. The aim is to understand the effects of the different modifications applied to the combustor unit, insulation of the compressor and expander units, and intercooling load on the characteristics of the entire powertrain. Assessment of the potential of the DICI H_2 combustion concept combined with the split-cycle engine is performed, and likely efficiency levels of the entire powertrain are estimated. The DCEE fueled with H_2 is also compared to that fueled with conventional diesel.

This paper first provides details of the combustion cylinder (the base diesel engine) and its operating conditions, as well as the different generations of the DICI H_2 combustion system considered (Section 2). Then, a description of the 1D GT-Power model of the entire DCEE system is given in Section 3. Subsequently, the results of the study are presented and discussed in Section 4, where the different generations of the DICI H_2 combustion concept and the CDC are compared in terms of system thermodynamic parameters, energy losses, and efficiency. Effects of the charge air cooler and compressor and expander insulation are investigated in Sections 4.2 and 4.3, respectively. Finally, the benefits of DICI H_2 combustion compared to the CDC in the context of the DCEE are summed up in Section 4.4, while Section 5 summarizes the conclusions

of this work.

2. Combustion cylinder specifications and operating conditions

As mentioned in Section 1, the combustor unit of the DCEE is essentially a combustion cylinder of a conventional CI diesel engine with a single major modification – a lower compression ratio piston. Hence, the base engine used for simulations and experiments is a single-cylinder variant of a standard heavy-duty low-swirl Volvo D13 diesel engine. An H_2 high-pressure injector was then computationally incorporated into the base engine, which was thoroughly studied in [8–10]. The H_2 high-pressure injector nozzle geometry used in these CFD studies was based on a commercial HPDI natural gas injector [12]. The rest of the combustion system was left unchanged in the first generation of the DICI H_2 concept compared to the diesel variant.

The DICI H_2 engine in this work is first compared to the conventional diesel combustion (CDC) engine. Two CDC cases are considered, reference CDC and high-T CDC. The former is based on the original diesel combustion cycle data experimentally measured in [6] (56.9 bar FuelMEP). It was also used to validate the engine CFD model. The high-T CDC, on the other hand, has operating conditions modified from the original case for a better comparison with DICI H_2 combustion. The modifications include raised in-cylinder temperature at IVC (hence the name), and, therefore, slightly altered IVC pressure and gas composition. The DICI H_2 combustion, in turn, required raised IVC temperatures for an easier ignition of H_2 fuel, and higher EGR rate (Eqn. (1)) to match global equivalence ratio with the CDC. The base engine specifications and operating conditions for the two diesel and the first-generation H_2 combustion cases are given in Table 1. The specifications of the other four generations of the DICI H_2 combustion concept are given Fig. 2.

Gen. 1 case serves as a starting point with minimum modifications to the original diesel case (only different injector). Gen. 3 is one of the "optimized" [a] cases with improved piston geometry and injector

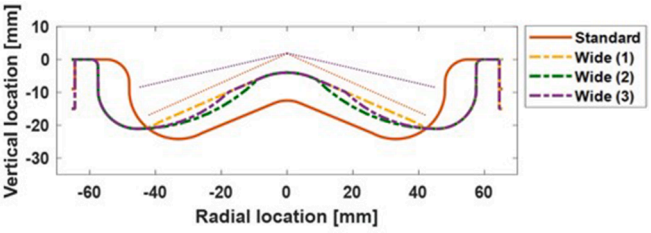

DICI H_2 combustion	Bowl type	Nozzle orifice #	Orifice diameter	Umbrella angle	Injection pressure
Gen. 1	Standard	7	1 mm	132°	300 bar
Gen. 2	Wide (1)	7	1 mm	154°	300 bar
Gen. 3	Wide (2)	12	0.76 mm	154°	300 bar
Gen. 4	Wide (3)	12	1 mm	154°	220 bar
Gen. 5	Wide (3)	12	1 mm	154°	300 bar

Fig. 2. Specifications of the different generations of the DICI H_2 combustion concept tested in this work.

umbrella angle, increased number of nozzle orifices, and reduced orifice diameter for maintaining the original injector flow rate capacity. Equivalence ratio in all H_2 cases is set equal to that of the High-T CDC via adjusted EGR rates for the sake of comparison (neither are optimum for H_2). Gen. 4 is the other "optimized" case that achieves the same goals as Gen. 3 but instead of the reduced orifice diameter, the injection pressure is lowered to maintain original injector flow rate capacity. Finally, Gen. 5 is used to test the effects of increased injection flow rate, thus it has both the original injection pressure (300 bar) and nozzle orifice diameter (1 mm), and a larger number of orifices (twelve).

The effects of the described modifications on the distribution of energy flow components in the engine cylinder (useful work versus losses) are shown in Fig. 3. Note that these results are for the combustor unit

Table 1
Base research engine specifications and operating conditions.

	Reference CDC	High-TCDC	DICI H_2(Gen. 1)
Cylinder bore	131.0 mm		
Stroke	158.0 mm		
Con. Rod length	267.5 mm		
Crank offset	0.0 mm		
Compression ratio	11.5: 1		
Fuel system	Common-rail direct-injection		
Nozzle orifice #	7	7	7
Orifice diameter	0.265 mm	0.265 mm	1 mm
Injector umbrella angle	145°	145°	132°
Injection pressure (main and pilot)	2200 bar	2200 bar	300 bar
Pilot injection timing	–	–	−10 CA° aTDC
Pilot injection duration	–	–	70 μs (0.5 CA° at 1200 RPM)
Pilot injection target fuel mass	–	–	1.5 mg
Main injection timing	−3 CA° aTDC	−3 CA° aTDC	0 CA° aTDC
Main injection duration	1500 μs (10.8 CA° at 1200 RPM)	1500 μs (10.8 CA° at 1200 RPM)	1300 μs (9.4 CA° at 1200 RPM)
Main injection fuel mass	275.6 mg	275.6 mg	99.5 mg
FuelMEP	56.9 bar	56.9 bar	56.9 bar
EGR rate	40%	40%	48%
Global air-fuel equivalence ratio (λ)	1.36	1.17	1.17
In-cylinder pressure at IVC [a]	6.8 bar	7.1 bar	7.0 bar
In-cylinder temperature at IVC [a]	446 K	528 K	528 K
Piston temperature [a]	800 K	800 K	800 K
Cylinder liner temperature [a]	610 K	610 K	610 K
Cylinder head temperature [a]	740 K	740 K	740 K
Engine speed	1200 RPM	1200 RPM	1200 RPM
	In-cylinder composition at IVC (mass fractions) [a]		
O_2	0.1563	0.1413	0.1272
N_2	0.7416	0.7478	0.7762
CO_2	0.0696	0.0803	–
H_2O	0.0325	0.0307	0.0966

[a] Estimated using 1D GT-Power simulations.

only. The results demonstrated the effectiveness of the adopted optimization strategy, where gross indicated efficiency increased by up to 2.9%-points (Gen. 5 compared to Gen. 1), while heat transfer losses reduced by up to 35.3% (Gen. 4 compared to Gen. 1).

Even though incomplete combustion losses tend to increase with the adopted strategy, additional optimization of the piston and injector designs may alleviate this issue [10]. Moreover, the unburned H_2 exiting the combustor unit of the DCEE will eventually oxidize on the catalyst in the HP tank, thus providing additional energy for the expander unit to convert to work and partly offset the loss.

The EGR rate is defined according to Eqn. (1):

$$\mathrm{EGR_{rate}} = \frac{m_{EGR}}{m_{air} + m_{EGR}} * 100\ \% \tag{1}$$

where, m_{EGR} is cycle-average EGR mass flow rate and m_{air} is cycle-average fresh air mass flow rate. The fresh air is assumed to be dry, while EGR is assumed to be saturated (after the EGR cooler).

In the following, all cases described above are computationally incorporated into the DCEE combustor unit using a 1D GT-Power model, the details of which are given in Section 3. Note that the DICI H_2 Gen. 2 case is omitted in this analysis because it is merely a transitional case that was only used for comparison in the previous study, hence is not interesting for the purposes of the current work.

3. 1D GT-Power model description

3.1. DCEE model components

The layout of the 1D GT-Power model used in the analysis is presented in Fig. 4. It consists of the compressor, combustor, and expander units, each represented by an engine cylinder object. Each unit is connected to a single engine cranktrain mechanism. Operation of the compressor and expander are offset by -90° and $+90^{\circ}$, respectively, relative to the combustor phasing. The former two are two-stroke machines, whereas the latter one is four-stroke. The physical dimensions of each unit are given in Table 2. Note that the bore of the compressor and expander is set to an optimum value for each case separately. This is to enable fair comparison because, in reality, the engine would be optimized differently depending on the combustion concept chosen. Also

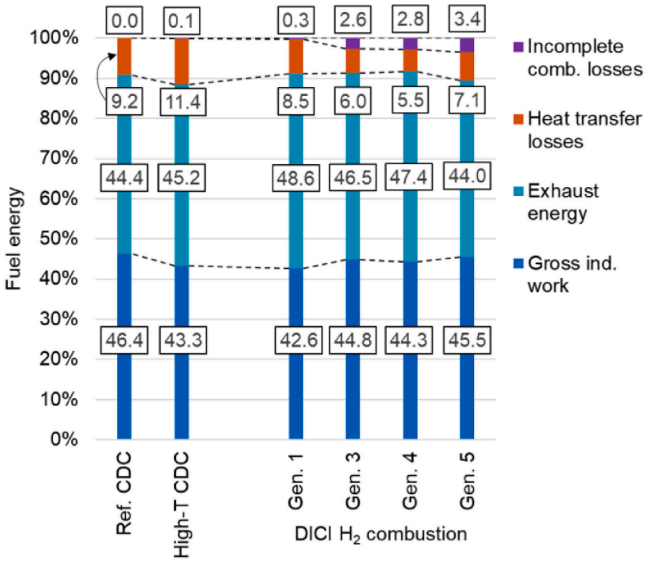

Fig. 3. Fuel energy distribution between gross indicated work, exhaust energy, wall heat transfer, and incomplete combustion losses in the combustor unit of the DCEE with different combustion concepts [10]. The results are from 3D CFD simulations of the combustion cylinder only.

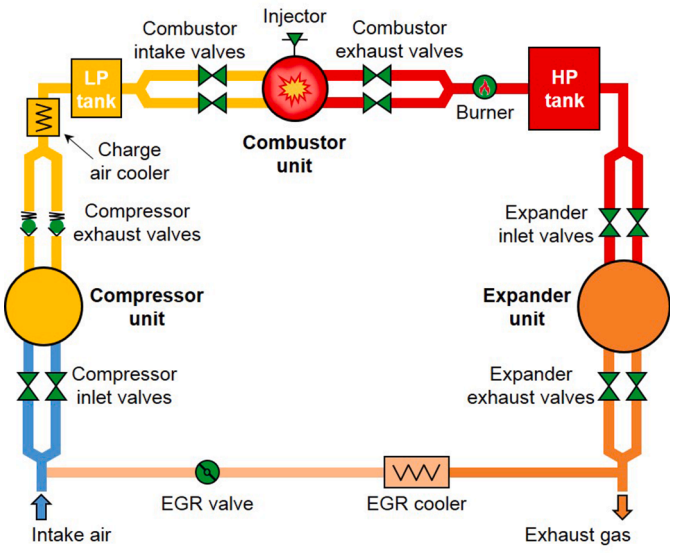

Fig. 4. Layout of the DCEE system used in 1D GT-Power model.

Table 2
Specifications of each dedicated unit of the baseline DCEE.

	Compressor	Combustor	Expander
Bore [mm]	170 [c], 180 [d]	131	225 [e], 230 [f]
Stroke [mm]	158	158	158
Compression ratio [-]	159	11.7	159
Displacement [L]	3.6 [c], 4.0 [d]	2.13	6.3 [e], 6.6 [f]

[c] For Reference CDC.
[d] For High-T CDC, and DICI H_2 Gen. 1, 3, 4, and 5.
[e] For Reference CDC, High-T CDC, and DICI H_2 Gen. 5.
[f] For DICI H_2 Gen. 1, 3, and 4.

note that, the expander unit displacement is set such that the pressure at EVO is equal to ~1.3 bar in all cases. This value is a compromise between the useful work production and the anticipated friction loss in the expander.

The LP and HP accumulator tanks are assumed to be 32.4 L cylinders, large enough to dampen any large pressure fluctuations. The diameter of the pipes connecting the different components of the system is set at 130 mm before the LP tank, 85 mm between the LP tank and the intake ports of the combustor unit, 48 mm between the exhaust ports of combustor unit and the HP tank, and 130 mm after the HP tank.

In this work, the HP tank is assumed to incorporate an oxidation catalyst in cases where the percentage of unburned H_2 after the combustor unit is significant. This would reduce a potential H_2 slip, as well as provide more energy for the expander unit to convert into useful work. The exhaust gasses of the combustor unit are expected to reach temperatures of 600–800 °C, which are likely too high for selective catalytic reduction (SCR). Thus, a catalytic combustor may be incorporated inside the HP tank, while an SCR catalyst (if needed) may be installed downstream of the expander unit where temperatures are much lower. Oxidation catalysts based on metal oxides would likely be favored in our case because of their lower cost and higher thermal stability compared to noble metal catalysts [13]. The typical drawbacks of the solid oxide catalysts, such as the lower specific activity and, consequently, higher ignition temperature, would be avoided owing to the high temperatures in the HP tank. For NOx emissions control, H_2 could be used instead of ammonia as a reducing agent in the SCR system, which would help avoid urea and byproduct deposition, and the need for

an extra tank and ammonia slip catalyst [14]. Finally, the exhaust gas temperatures after the expander unit would also be lower in the DCEE compared to conventional engines, which could enable high N_2 selectivity and improved NOx conversion efficiency.

In the 1D model presented in Fig. 4, the oxidation catalyst is represented by a burner object located just upstream of the HP tank object.

3.2. Heat transfer modeling

Heat transfer in all cylinders is modeled with the WoschniGT model [11], which is based on [15]. Heat transfer in the ports and pipes, on the other hand, is modeled using the Colburn correlation [16,17]. The model is based on the Colburn analogy, which is known to be the most accurate among other heat, momentum, and mass transfer analogies, and is generally valid for fully developed turbulent flows in conduits. Heat transfer multipliers (HTMs) are commonly used to customize the heat transfer correlations to achieve a better fit to available data. They appear as simple multipliers in the convective heat transfer coefficient equation of the Woschni and Colburn models. Radiation heat transfer is assumed proportional to the combustion term, and hence lumped into the convection equation. This assumption is justified because a change in radiation is largely due to a change in emissivity of the flame, which is approximately proportional to the input fuel rate [15].

3.2.1. Compressor unit

Heat transfer in the compressor cylinder is calculated using the Woschni correlation. The piston temperature is set at the cylinder oil temperature of 360 K for all cases, which is equal to the experimentally measured oil temperature for the diesel case. The cylinder liner and head temperatures are set to be equal to the measured coolant temperature of 355 K. Convection and radiation heat transfer multipliers of 1.0 are selected for the compressor unit as the most reasonable assumption, for lack of more accurate data. The multipliers are changed to 0.1 in the cases with insulated compressor.

Heat transfer in the inlet and exhaust ports and manifolds of the compressor unit is modeled using the calculated wall temperature method, where it depends on the port material and coolant temperature. The Colburn heat transfer correlation is adopted in the model.

3.2.2. Combustor unit

In all simulated cases, the combustor unit's piston, liner, and head temperatures are set at 800 K, 610 K, and 740 K, respectively. These values are taken from the 3D CFD simulations for consistency, which in turn were estimated from experimental data. Note that these values are higher than the typical wall temperatures found in the standard Volvo D13 engine. This is justified by the higher cycle-average combustor gas temperatures and the less effective cooling of the piston, caused by the low compression ratio piston of the DCEE, at 11.5:1 (compared to 17:1 in the standard engine). The modeling results are, however, only sensitive to the piston temperatures due to the much higher incident velocities and near-surface temperatures compared to those for the liner and head.

The convection heat transfer multiplier is set at different values, depending on the temporal location within the cycle, and adjusted to fit the wall heat flux profile obtained via 3D CFD. The separate treatment of the compression and expansion strokes was necessary because of the large differences in heat release traces, injection and jet momentum, and hence near-wall gas velocities and temperatures during the expansion stroke of the different cases considered, while the differences during the compression stroke were not as large and did not necessarily follow the same trends. The HTMs during the intake and exhaust strokes are assumed to be equal to those during the compression and expansion strokes, respectively; however, the results of the simulations were also found to be insensitive to these values. The fitted multipliers are given in Table 3 (left side). Note that the DICI H_2 cases have lower multipliers than the CDC during expansion, which reflects the lower heat transfer losses estimated with 3D CFD, as shown in Fig. 3. Table 3 (right side) also shows that, if heat transfer multipliers in 1D GT-Power simulations were not adjusted to fit 3D CFD data, the total wall heat transfer loss would be significantly overpredicted, especially with DICI H_2 combustion cases. On the other hand, the radiation heat transfer multiplier of the combustor unit is set at 1.0 for all cases for the entire cycle.

Table 3
(Left side) Combustor unit's convection heat transfer multipliers (HTMs) fitted to 3D CFD data and (Right side) the total wall heat transfer loss until EVO estimated in 3D CFD simulations, 1D GT-Power with HTM of 1.0, and 1D GT-Power with fitted HTMs.

	Fitted HTMs [-]		Total wall heat transfer loss [J]		
	Int. + Comp. strokes	Exp. + Exh. strokes	3D CFD	1D GT (HTMs = 1.0)	1D GT (fitted HTMs)
Reference CDC	0.47	0.96	1086	1167	1068
High-T CDC	0.40	1.06	1326	1354	1333
DICI H_2 Gen. 1	0.40	0.81	997	1215	984
DICI H_2 Gen. 3&4	0.60	0.40	625	1200	622
DICI H_2 Gen. 5	0.60	0.55	832	1331	827

Heat transfer in the inlet and exhaust ports of the combustor unit is modeled using the imposed wall temperature method. The wall temperatures are set according to experimentally measured values of 367 K and 406 K for the intake and exhaust ports, respectively. The heat transfer multiplier for the intake ports is set at 1.5, while that for the exhaust ports is either 1 or 0, depending on the case (uninsulated- versus insulted-port cases). Heat transfer in the intake and exhaust manifolds, on the other hand, is modeled using the calculated wall temperature method, like with the compressor unit.

3.2.3. Expander unit

Heat transfer modeling in the expander unit is performed in a slightly different manner. Instead of specifying wall temperatures directly, a finite-element cylinder wall temperature solver is implemented in GT-Power, with specified geometrical and material parameters of the piston-cylinder-head assembly and the adjacent valves and ports. Both the convection and radiation heat transfer multipliers are set at 1.0, unless the expander is assumed insulated, in which case the multipliers are set at 0.1.

Heat transfer in the inlet ports and manifold of the expander unit is set to zero (adiabatic), assuming their perfect insulation. Heat transfer in the exhaust ports of the expander unit is modeled using the imposed wall temperature method (450 K) and Colburn correlation, while exhaust manifold is modeled using the calculated temperature method.

3.3. Friction modeling

Friction loss estimation in this work is performed by adopting a simple FMEP model – a linear function of the peak cylinder pressure. This correlation is adopted from [6], and presented in Eqn. (2):

$$\mathrm{FMEP} = \frac{C_1}{C_2}\mathrm{PCP} \tag{2}$$

where, FMEP is a friction mean effective pressure, PCP is peak cylinder pressure (during combustion), C_1 – first correlation coefficient (set at 1.2), C_2 – second correlation coefficient (set at 200). The choice of this model is predicated on the observation that the FMEP correlates strongly with the maximum PCP capability of the engine design, as concluded in [6,18–20]. This may be explained by the need for larger bearings, higher levels of piston ring tension, and overall, more robust and heavy-duty structure of the engine operating at higher PCPs. Fig. 5 illustrates the

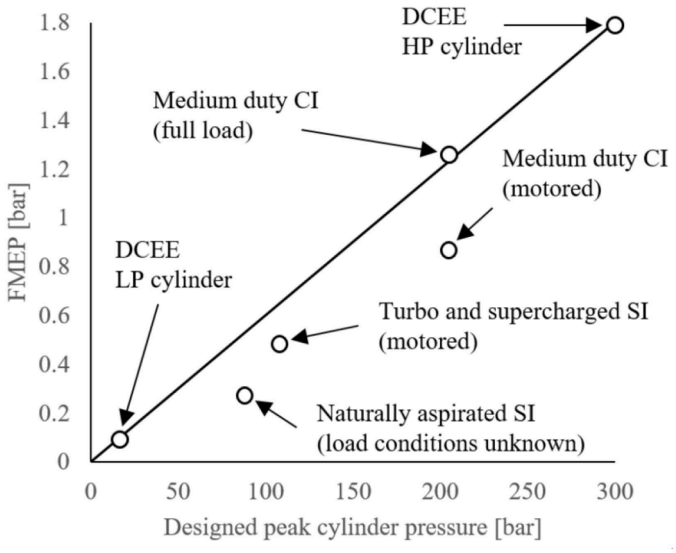

Fig. 5. Linear FMEP correlation [6] adopted in this work in comparison to the measured FMEP values reported in [18–20].

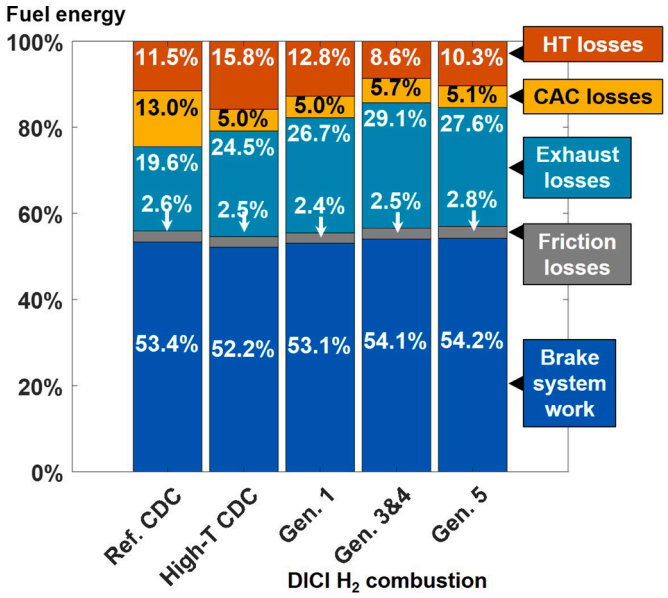

Fig. 6. Fuel energy distribution between brake system work, friction, exhaust, charge air cooler (CAC), and heat transfer (HT) losses for the reference CDC, high-temperature CDC, and DICI H_2 Gen. 1, Gen. 3&4, and Gen. 5 cases with insulated exhaust ports of the combustor unit.

adopted FMEP correlation, along with the measured values from the literature. It is observed that this approach yields conservative estimations of the friction losses.

3.4. 1D model calibration

The 1D model of the DCEE is calibrated against the experimentally validated 3D CFD simulation results from the previous study [10]. The closed-volume combustion cycles obtained from CFD are imposed in the combustor unit of the DCEE. The models are calibrated against all operating points using the following metrics:

1 In-cylinder pressure and chemical heat release
2 In-cylinder mean temperature
3 Total heat loss to all cylinder walls before EVO
4 Pressure and temperature at IVC
5 Pressure and temperature at EVO
6 Trapped in-cylinder mass
7 Global equivalence ratio

The calibration is performed by adjusting the displacement of the compressor and expander units, convection heat transfer multipliers at different stages in the cycle, expander IVC timing, and cooling load of the charge air cooler. An example of the pressure trace obtained with the calibrated 1D model in comparison to the 3D CFD and experimental data is given in the Appendix (Figure A1).

4. Results and discussion

4.1. Baseline DCEE system efficiency and losses

Results of the entire DCEE system simulations are presented and discussed in this section. Fig. 6 shows the fuel energy distribution between the brake useful system work, friction, exhaust, charge air cooler, and heat transfer losses for the CDC and DICI H_2 combustion cases. Note that the incomplete combustion losses are not included in this chart because all unburned fuel is assumed to have oxidized in the catalyst incorporated inside the HP tank. This is another advantage of the DCEE design, in which incomplete combustion losses are partly recovered in the expander to produce more work, such that the exhaust losses are minimized.

Brake system work, which taken as a percentage of the fuel energy input, is equivalent to the brake thermal efficiency (BTE) of the powertrain, is the highest with DICI H_2 Gen. 5, followed closely by Gen. 3 and 4. Heat transfer losses in the entire system are significantly lower with the Gen. 3–5 cases, which is expected since combustor is the dominant contributor to the total heat transfer losses in the system, and combustor heat transfer is substantially lower with "optimized" DICI H_2 combustion.

The amount of heat rejected via the charge air cooler is larger with the DICI H_2 cases compared to the equivalent CDC (High-T – with equal peak motoring temperature). This is explained by the higher in-cylinder pressures and temperatures at EVO (see Fig. 7), which lead to a larger amount of in-cylinder residual gasses at higher temperatures after the end of the exhaust stroke. As a result, the cooling load on the CAC must also be raised.

Friction losses for all cases are fairly low and relatively equal.

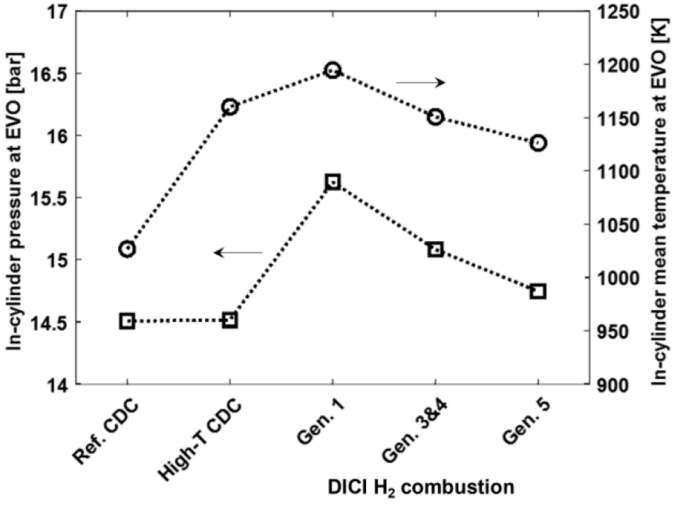

Fig. 7. In-cylinder pressure and temperature at exhaust valve opening (EVO) for the CDC and DICI H_2 combustion cases.

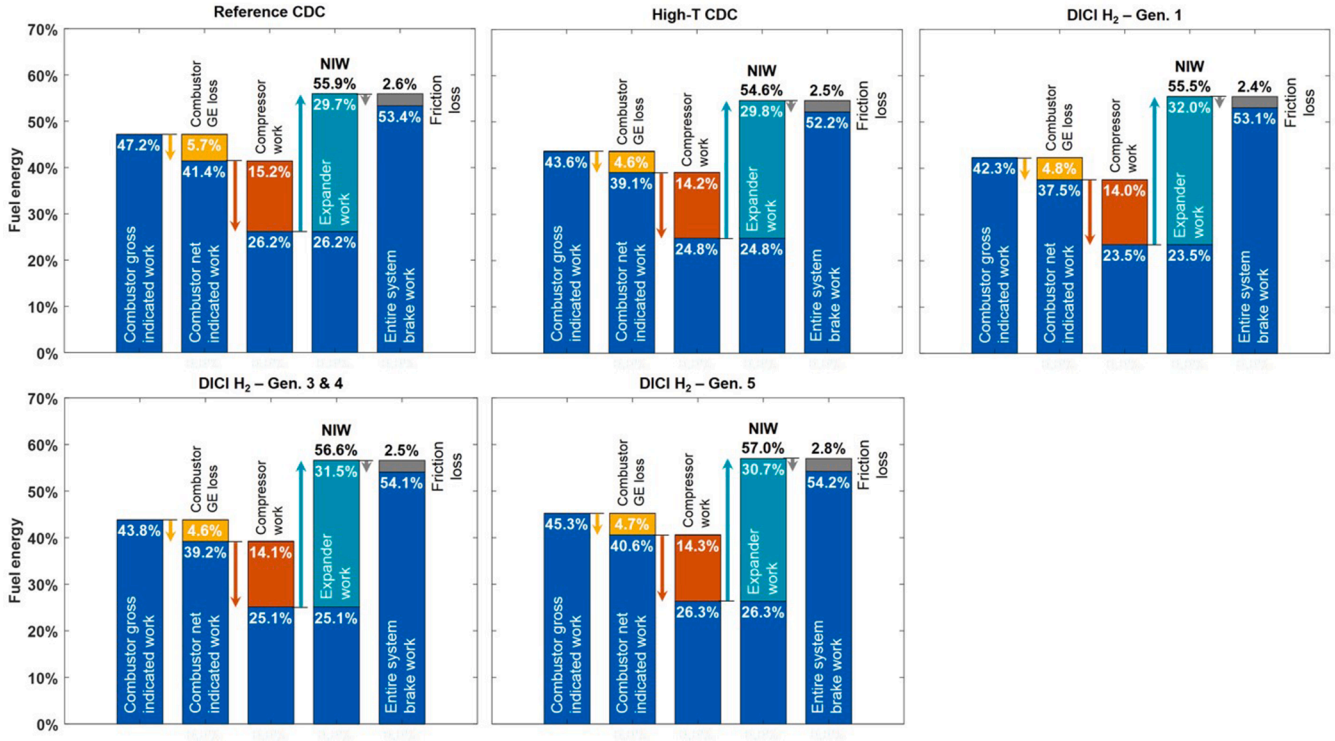

Fig. 8. Engine energy flow from compressor to expander of the DCEE concept with the reference CDC, high-temperature CDC, and DICI H_2 Gen. 1–5 combustion cycles in the combustor unit with insulated exhaust ports.

Combustor unit is responsible for most of the friction losses, at 93.3% for the Ref. CDC case. Compressor and expander units account for only 2.9% and 3.8% of the total friction losses, respectively. The FMEP of the combustor unit, which is the dominant component contributing to friction losses, is estimated to equal 1.24 bar for the Ref. CDC case. The estimations hold well against experimentally measured values from the literature for medium- and heavy-duty CI engines operating at 1200 RPM, peak cylinder pressures of around 200 bar, and high engine load conditions [18–23]. The friction losses can be further reduced by using larger compressor and expander units while operating the combustor unit at an even higher load point.

The exhaust losses for the DICI H_2 cases are higher than those for diesel, which is the result of the generally higher combustor EVO pressures and temperatures (see Fig. 7), reduced intercooling, and larger amount of unburned fuel in the combustor cylinder of the DCEE, which ends up oxidizing later in the DCEE cycle. Note that the relative distribution of fuel energy between the exhaust losses and brake system work cannot be explained based on Fig. 6, thus another type of analysis is performed and discussed in the following.

Fig. 8 presents the distribution of fuel energy in the form of engine energy flow, starting from the work produced in the combustor unit, followed by the loss of work due to gas exchange in the combustor unit, and compression process in the compressor unit. This is followed by production of useful work in the expander unit and destruction of potential work due to friction losses, finally arriving at the brake work output of the entire system. Note that the combustor gross indicated efficiencies (GIE) reported in this section do not necessarily match the GIEs presented in Section 1 because of the limitations of the closed-cycle CFD simulations in the latter, where the parts of the cycle before the IVC and after the EVO were reconstructed using an isentropic relation. This is, however, not the case in the current section, where the actual gas exchange process is modeled, which yields slightly different combustor GIE values. It should be emphasized that, despite the discrepancies, the thermodynamic cycle parameters obtained from the 3D and 1D simulations still match during the closed-volume phase, as discussed in Section 2.4.

Fig. 8 shows that, even though, the slower heat release of the High-T CDC results in a lower gross work from the combustor unit compared to the reference CDC, the BTEs of the entire DCEE system are still comparable. This is because the work lost in the combustor is compensated with a lower negative compressor work and intercooling loss, the latter of which is included in the gas exchange component. The negative compressor work is lower due to the compressor's smaller size, which could be reduced owing to the smaller heat loss in the low-pressure part of the DCEE (before the combustor unit), which would otherwise lead to higher pressures for the same cylinder displacement. This showcases an important advantage of the DCEE system being insensitive to the intake temperatures, which enables an efficient operation with high octane number fuels that require high temperatures for autoignition, such as hydrogen and potentially methane, methanol, ammonia, etc.

Compared to high-T CDC, Fig. 8 also shows that the useful work produced by the expander unit is larger for the DICI H_2 cases. This is because of the lower combustor heat transfer loss and higher exhaust pressures and temperatures, which is also consistent with the energy distribution diagram presented in Fig. 3. An exception is Gen 5, which still has a relatively high expander work despite having lower combustor exhaust energy. This is explained by the relatively large amount of unburned fuel in the combustor unit being oxidized on the catalyst in the HP tank, thus adding more energy to the expander unit. Gen. 5 also has the highest BTE, which suggests that optimization of the combustor unit is more important than that for the rest of the DCEE system.

4.2. *Intercooling losses*

The charge air cooler (CAC) is used in the DCEE to ensure high volumetric efficiency and low gas specific heat ratio for the combustor unit, which effectively led to an overall improved performance of the DCEE [24]. However, the benefits of intercooling on the burning rate

Table 4
DCEE system parameters with and without intercooling (CAC) for the reference CDC and DICI H_2 Gen. 3&4 cases, with no restrictions on the combustor inlet pressures.

	Reference CDC		DICI H_2 Gen. 3&4	
	With CAC	Without CAC	With CAC	Without CAC
Combustor inlet T [K]	333.81	528.81	421.19	514.21
Combustor inlet P [bar]	5.10	7.14	5.49	6.41
Combustor global λ	1.368	1.362	1.202	1.198
Combustor trapped mass [mg]	10,201.94	9997.75	8415.76	8379.78
Combustor PMP [bar]	147.66	185.68	148.91	166.44
Combustor PCP [bar]	206.61	231.17	200.75	213.53
HP tank and Expander inlet T [K]	899.89	1007.26	1022.27	1074.93
HP tank and Expander inlet P [bar]	7.74	8.37	7.63	8.18
Expander T_{EVO} [K]	547.27	623.88	627.92	657.87
Expander P_{EVO} [bar]	1.19	1.35	1.23	1.28

and heat transfer losses in the combustor unit were previously shown to be insignificant. One of the limitations of the previous analyses was the assumption of constant inlet pressures, and hence peak motoring pressures of the combustor unit, regardless of the level of intercooling. If the pressure is allowed to change freely with the intercooling load, then the effects of the increased CAC load on the efficiency of the DCEE are not always positive. This is because intercoolers not only lower the inlet air temperature, but also the pressure (consider the ideal gas law).

A parametric study of the effects of the CAC on the DCEE system losses with and without the restrictions on the combustor peak motoring pressures is carried out in this work. Table 4 reports the important system parameters affected by the removal of intercooling. Some notable effects are the increase in the temperatures and pressures in the combustor inlet manifold, HP tank and expander inlet manifold, while the global equivalence ratio in the combustor unit remained unchanged. Fig. 9 (w/o CAC), compared to Fig. 8 (with CAC), shows that, as concluded in [24], the combustor indicated efficiency is lower when no intercooling is applied (w/o CAC), and the negative compressor work is higher as a result of the higher LP tank pressures. However, the improvements in the positive expander work offset the drawbacks upstream of the expander, leading to a 0.2%-points higher BTE of the entire system without the CAC. Expander work improvements are the result of the higher HP tank pressures and temperatures, which in turn, arise from the overall increased combustor pressures and temperatures (see Table 4).

The combustor pressure level could also be increased without removing the CAC; however, this would require a larger compressor unit, hence more negative compression work. As shown in Appendix (Figure A2 (top right) and Table A1), the tradeoff would overall be unfavorable. Removing the intercooling but restricting the combustor inlet pressure would, on the other hand, yield lower combustor and expander work output, which should also be avoided (Figure A2 – bottom left).

Gen. 3 and 4 of the DICI H_2 combustion system were selected to perform similar type of analysis on the effects of the CAC. Comparing Fig. 9 (bottom plot) with Fig. 8, similar conclusions to those with the CDC are drawn. Despite the lower combustor indicated efficiency and higher negative compressor work, the system BTE is 0.5%-points higher without intercooling, as a result of the significantly increased expander positive work.

Considering the higher PMP in the combustor unit for the non-intercooled cases, the effective compression ratio of the entire DCEE (defined according to Eqn. (3)) is also higher, at around 43:1 instead of the previous 39:1 for Gen. 3 and 4, despite the unchanged compressor or combustor specifications. Thus, the tradeoff between the positive effects of the higher system effective compression ratio and the negative effects

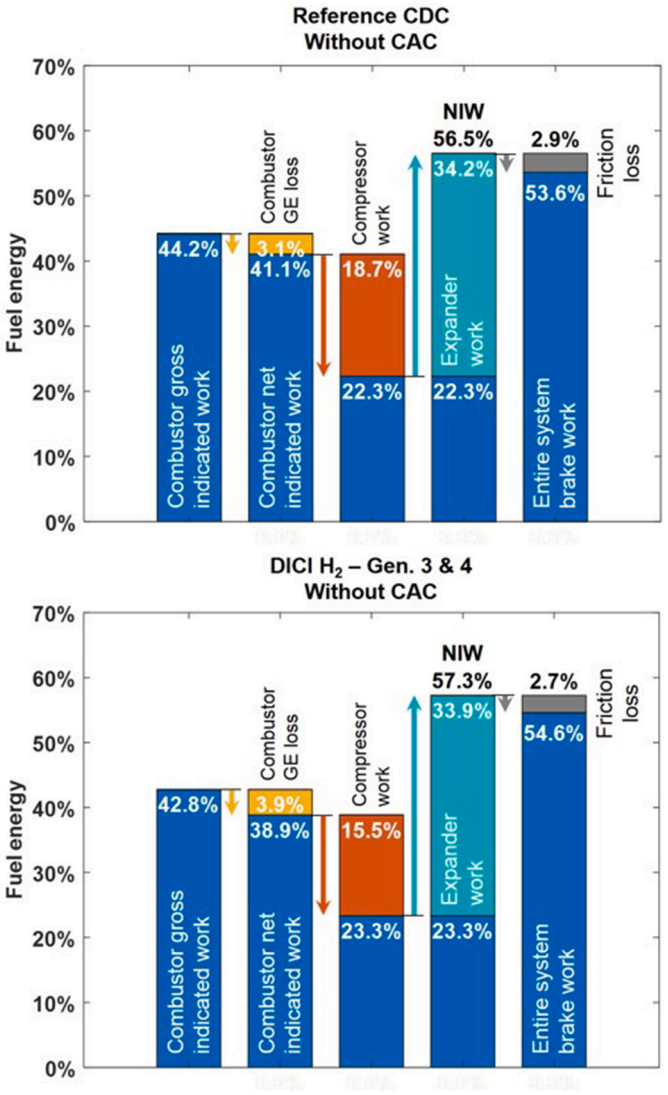

Fig. 9. Engine energy flow from compressor to expander of the DCEE concept with the reference CDC and DICI H_2 Gen. 3&4 combustion cycles in the combustor unit with insulated exhaust ports and without the charge air cooler.

of the higher combustor inlet temperature (see the first paragraph of this section) favors the former. Furthermore, considering the need for higher combustor inlet temperatures for easier ignition of H_2, it is concluded that the removal of intercooling is desirable for H_2 fueled DCEE.

$$CR_{eff} = \left(\frac{PMP}{P_{in}}\right)^{\frac{1}{\gamma}} \tag{3}$$

where, PMP is peak motoring pressure in the entire cycle (at TDC of the combustor unit), P_{in} is intake pressure into the DCEE system (before compressor), and γ is specific heat ratio of the gas being compressed (= 1.36 with EGR).

Note that the HP tank and expander inlet temperatures also increased quite significantly with the removal of intercooling, reaching especially high values with the DICI H_2 combustion cases, as seen in Table 4. Temperatures in the range of 1000 K may cause thermal corrosion of the HP tank materials. Solutions to this issue may include the use of different metal alloys and/or more dilute operation of the combustor unit. Considering that the former option will increase the price of the powertrain, the latter is more appealing, especially in the case of H_2 combustion, which owing to the different stoichiometry, may be

implemented at a higher λ while keeping the same EGR ratio. On the other hand, the higher HP tank temperatures could allow the use of cheaper oxidation catalysts based on metal oxides, which would perform better than noble metal catalysts at these conditions (see Section 2.1).

The higher pressure levels in the combustor unit may also impose more strict requirements on the gaseous fuel injection system, thus a careful consideration of the tradeoffs should be carried out before the future attempts on further system optimization.

4.3. Compressor and expander insulation

Compressor and expander units of the DCEE were specifically designed to allow their effective insulation. This involves unique valve design, flat cylinder heads, and the use of temperature "swing" coating on the piston [25,26]. Note that, because there is no fuel injection or combustion in the expander unit, the usual challenges associated with the use of temperature "swing" coatings, such as unburned hydrocarbons and buildup of soot, would not be faced in the expander unit of the DCEE, thus increasing their effectiveness and ease of use. The use of H_2 as fuel further simplifies implementation of the thermal swing technologies.

In the current 1D study, to simulate the effects of insulation on the compressor and expander units, the heat transfer multipliers (both convection and radiation) in these components of the model are set at 0.1 instead of the usual 1.0. The results of these simulations are presented in this section. Note that the heat transfer in the compressor unit is generally low due to its operating temperatures, as seen in Fig. 10. The heat transfer in some parts of the compressor cycle is from the coolant to the cylinder, thus recuperating most of the losses in the other parts of the cycle. Therefore, compressor insulation may be avoided taking into account additional costs. However, expander heat transfer is significant, in the range of 4% of fuel energy, hence expander insulation is justified.

The results of simulations with insulated compressor and expander units and no intercooling show a minor deterioration in the performance of the compressor and combustor units, which includes slightly larger negative compressor and gas exchange work (see Fig. 11 versus Fig. 9). However, the improvements in the positive expander work are much more significant, 1.6% and 1.7% of fuel energy for the reference CDC and DICI H_2 Gen. 3 and 4 cases, respectively. The improved expander performance is the result of not only reduced heat transfer losses in the expander itself, but also a more favorable ratio of pressure and temperature in the HP tank and expander inlet. As seen in Table 5, the HP

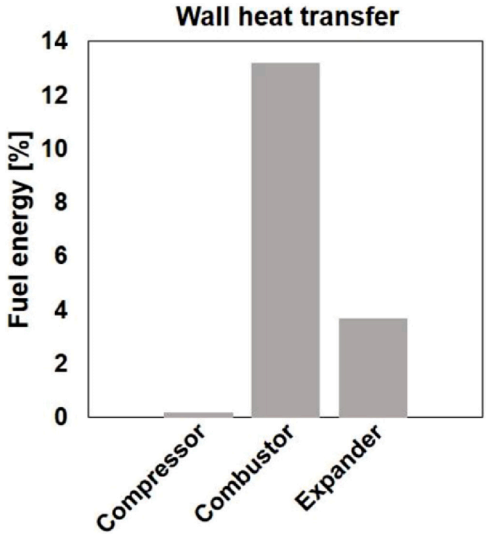

Fig. 10. Wall heat transfer as a percentage of fuel energy for the compressor, combustor, and expander units in the Reference CDC case without intercooling and cylinder insulation.

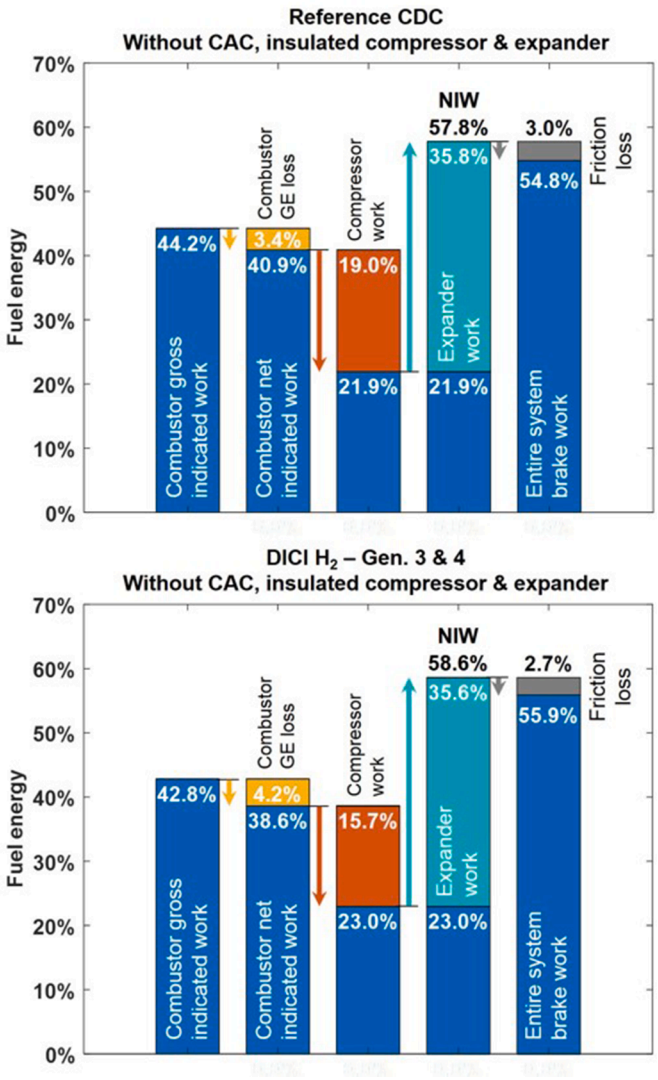

Fig. 11. Engine energy flow from compressor to expander of the DCEE concept with the reference CDC and DICI H_2 Gen. 3&4 combustion cycles in the combustor unit with insulated exhaust ports, assuming insulated compressor and expander units and no intercooling.

tank and expander inlet pressures increased with insulation, while the temperatures reduced, thus allowing less work to be lost to the exhaust. This is explained by the increased pressure in the high-pressure part of the system (after combustor), which carries through to the low-pressure

Table 5
DCEE system parameters with and without compressor and expander insulation for the reference CDC and DICI H_2 Gen. 3&4 cases, assuming no intercooling and no restrictions on the combustor inlet pressures.

	Reference CDC		DICI H_2 Gen. 3&4	
	Uninsul.	Insulated	Uninsul.	Insulated
Combustor inlet T [K]	528.81	530.89	514.21	514.95
Combustor inlet P [bar]	7.14	7.28	6.41	6.52
Combustor λ	1.362	1.398	1.198	1.214
Combustor trapped mass [mg]	9997.75	10,142.40	8379.78	8510.93
Combustor PMP [bar]	185.68	189.56	166.44	168.18
Combustor PCP [bar]	231.17	234.21	213.53	216.01
HP tank and Expander inlet T [K]	1007.26	1005.70	1074.93	1071.95
HP tank and Expander inlet P [bar]	8.37	8.63	8.18	8.43
Expander $T_{@EVO}$ [K]	623.88	648.66	657.87	686.17
Expander $P_{@EVO}$ [bar]	1.35	1.42	1.28	1.35

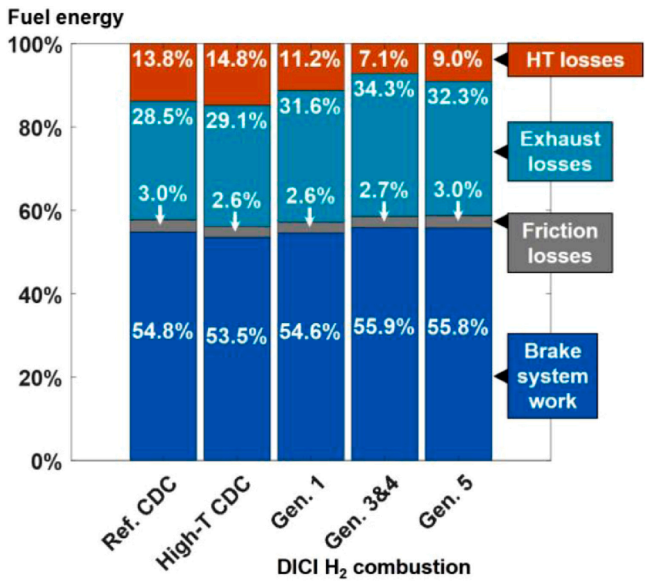

Fig. 12. Fuel energy distribution between brake system work, friction, exhaust, and heat transfer (HT) losses for the reference CDC, high-temperature CDC, and DICI H_2 Gen. 1, Gen. 3&4, and Gen. 5 cases with insulated compressor, expander, and exhaust ports of the combustor unit, and assuming no intercooling.

part, thus causing a higher λ in the combustor unit, which in turn, leads to the lower temperatures in the exhaust of the combustor and inlet of the expander.

As seen in Fig. 12, with insulated compressor and expander, and without the CAC, the DCEE, with all combustion concepts considered, has significantly lower heat transfer losses (cylinders + CAC), but higher exhaust losses, compared to the baseline variant. The tradeoff is overall positive, yielding the highest BTE of 55.9% with the DICI H_2 Gen. 3 and 4 cases. Thus, among all H_2 combustion cases considered, Gen. 3 and 4 are also the best, not only from the efficiency standpoint, but also because of their relaxed requirements on the fuel injection system, lower engine noise (compared to Gen. 5, see [10]), and likely lower NOx emissions (as will be further explored in a future study). Furthermore, the elimination of most of the incomplete combustion losses in the combustor unit should yield even higher BTE for the DICI H_2 combustion cases, even though it is not of the highest importance, owing to the possibility of H_2 oxidation in the HP tank.

It should be noted that insulation of the compressor and expander would not be as effective without removing the intercooling. As presented in Appendix (Figure A3), the deterioration of the expander performance would reduce the entire system efficiency by 0.5%-points, which is also consistent with the results from Section 3.2.

4.4. Benefits of hydrogen over diesel combustion

Along with the previous studies [8,10], the present work suggests that the DICI H_2 combustion has a greater potential than conventional diesel for modern engines like the DCEE for the following reasons. First, the non-premixed H_2 combustion approach offers more pneumatic work compared to the CDC. Even though H_2 combustion itself has a molar expansion ratio below unity (~ 0.85), the number of moles of H_2 fuel added near the TDC, due to its low molar mass, offsets the negative impact of the chemistry and leads to a large molar expansion, which is estimated to increase the IMEP by 1.2–2.4 bar or 2–4% of fuel energy in our case.

Second, the lack of soot emissions and high reactivity allow minimization of the intense momentum-dominated global mixing, typically used in modern diesel engines for a better soot-NOx tradeoff and faster heat release. The minimized global mixing enables significantly lower heat transfer losses in the combustion cylinder, which unlike the exhaust energy, cannot be effectively used in the expander unit or other waste heat recovery systems of modern engines. Unburned H_2 fuel in the combustion cylinder is also not as problematic as unburned diesel, due to the ease of hydrogen oxidation in the catalyst inside the HP tank, as well as, potentially, lack of associated pollutant formation. Additionally, a hydrogen DCEE may use an H_2-SCR instead of an NH_3-SCR, which would greatly simplify the system, as discussed in Section 2.1. The H_2-SCR could be installed downstream of the expander unit, where the DCEE would have lower temperatures compared to conventional diesel engines, thus enabling higher N_2 selectivity and improved NOx conversion efficiency.

As a result of the reduced heat transfer losses with minimized global mixing, improved heat release patterns, significant pneumatic work, and applied expander insulation with eliminated intercooling, the maximum brake thermal efficiency of the DCEE with the DICI H_2 combustion is expected to be around 56%. This is almost 2%-points higher than the DCEE with intercooling and limited insulation, and 1.1%-point higher that an equivalent DCEE fueled with conventional diesel fuel in the same load point (see Fig. 13).

Furthermore, with the current effective compression ratio of 43.3:1 with "optimized" Gen. 3 and 4 cases, the ideal Otto cycle efficiency is equal to 74.3%, assuming a constant specific heat ratio (γ) of 1.36 with the significant amount of water in the EGR. Thus, the DICI H_2 Gen. 3 and 4 cases, with the net indicated efficiency of 58.6%, currently achieve approximately 79% of the ideal Otto cycle efficiency. Due to a different stoichiometry of H_2 combustion, the H_2 engine may be operated at higher levels of dilution, either with air or EGR. Thus, additional optimization of the combustion system, such as adjusted λ and EGR and reduction of unburned H_2 in the combustor unit, are expected to further improve engine efficiency, reduce NOx and, potentially, heat transfer losses, without the typically associated increase in soot emissions.

Finally, DICI H_2 combustion allows for higher overall engine compression ratio compared to the SI mode, which enables the use of isobaric combustion [27–29] at pressures approaching the structural limitations of the engine (300 bar). This is also expected to significantly improve the system BTE.

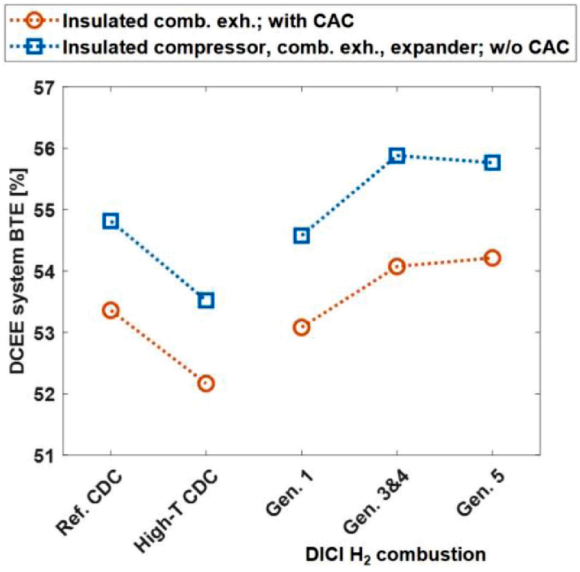

Fig. 13. Brake thermal efficiency of the entire DCEE system using the DICI H_2 combustion versus the CDC in the combustor unit with uninsulated and insulated exhaust ports.

5. Summary and conclusions

This study focused on incorporating a hydrogen (H_2) direct-injection compression-ignition (DICI) combustion concept into the double compression-expansion engine (DCEE) using a 1D GT-Power model. The aim was to understand the potential of the DCEE fueled with H_2 versus diesel, investigate the effects of intercooling and insulation, as well as to make predictions of likely efficiency levels of the entire system. The following are the conclusions of this work:

1 DICI H_2 combustion in modern engine concepts, such as the DCEE, may enable 56% brake thermal efficiency.
2 The DICI H_2 combustion shows a greater potential than the conventional diesel combustion because of the minimized heat transfer, which is possible owing to the lack of the soot-NOx tradeoff. This, combined with additional pneumatic work, results in at least 1%-point higher BTE with H_2 combustion compared to diesel. Further efficiency improvements are also expected with more optimization.
3 Among all the H_2 combustion system variants tested, those with the lower jet momentum and larger extent of free turbulent jet mixing (Gen. 3 and 4) showed the highest efficiency, mainly owing to the lowest heat transfer losses. They are also less demanding on the fuel injection system.
4 Removal of the intercooling improves the BTE by 0.5%-points but causes elevated temperatures in the high-pressure tank, which could make the selection of the tank material harder but also allows the use of cheaper oxidation catalysts.
5 Expander insulation gives additional 1.3%-points on top of the BTE improvements achieved by eliminating the intercooling, while compressor insulation proved inconsequential. The improved positive expander work is due to not only less heat transfer, but also more favorable ratio of pressure and temperature in the expander inlet.
6 The DCEE performance is insensitive to the combustion cylinder intake temperatures, thus making it potentially more suitable than conventional engines for use with high-octane fuels, such as hydrogen, methane, methanol, ammonia, etc., which require higher temperatures for autoignition.

Declaration of Competing Interest

The authors declare that they have no known competing financial interests or personal relationships that could have appeared to influence the work reported in this paper.

Acknowledgements

The authors would like to acknowledge financial support from the Combustion Engine Research Center (CERC) at Chalmers University of Technology and the Clean Combustion Research Center at the King Abdullah University of Science and Technology (KAUST).

Appendix A

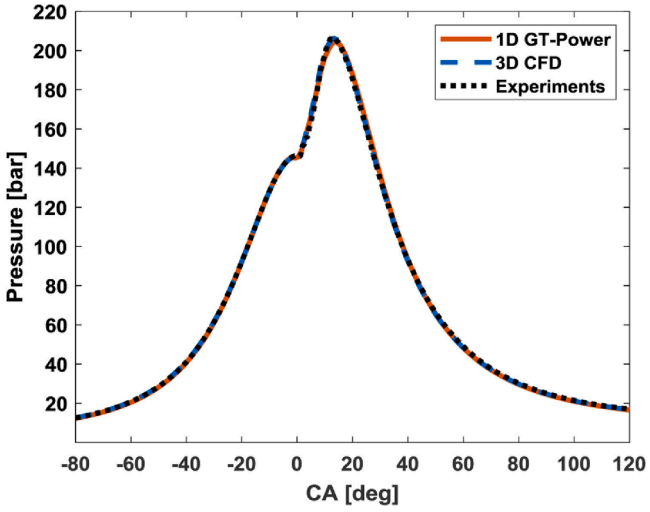

Fig. A1. Comparison of a typical in-cylinder pressure trace obtained using the 1D GT-Power model against 3D CFD and experimental data.

Table A1
DCEE system parameters obtained in the parametric study of the effects of the CAC, assuming the reference CDC in the combustor unit.

	With CAC		Without CAC	
	PMP w. CAC: unrestricted	PMP w. CAC≈PMP w/o CAC (unrestricted)	PMP w/o CAC≈PMP w. CAC (unrestricted)	PMP w/o CAC: unrestricted
Combustor inlet T [K]	333.81	332.85	497.88	528.81
Combustor inlet P [bar]	5.10	6.25	5.64	7.14
Combustor λ	1.368	1.890	1.099	1.362
Combustor trapped mass [mg]	10,201.94	12,880.82	8141.66	9997.75
Combustor PMP [bar]	147.66	185.96	145.32	185.68
Combustor PCP [bar]	206.61	239.44	198.32	231.17
HP tank and Expander inlet T [K]	899.89	787.73	1094.58	1007.26
HP tank and Expander inlet P [bar]	7.74	8.35	7.36	8.37

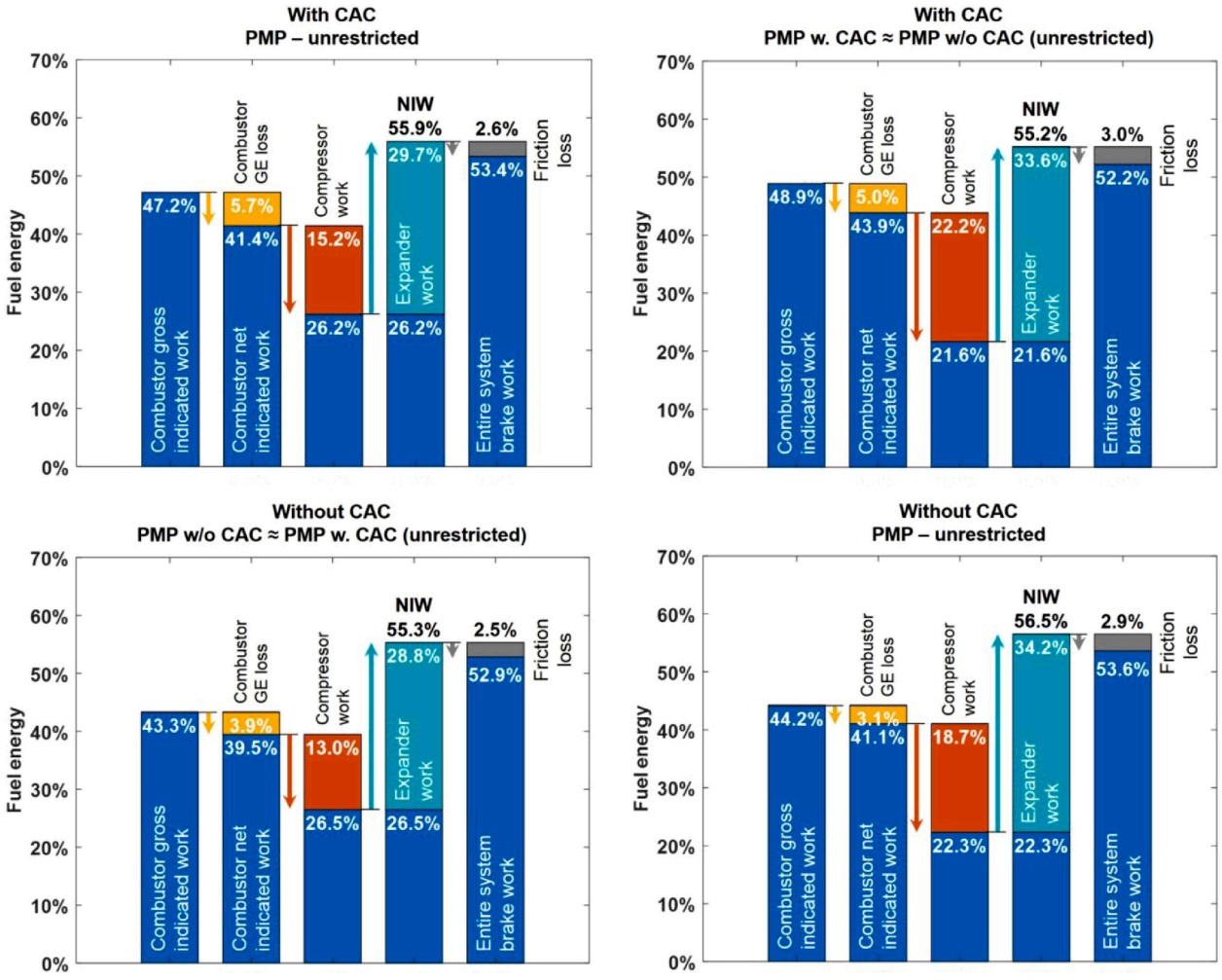

Fig. A2. Results of the parametric study for the effects of the CAC on the DCEE system losses and efficiency assuming reference CDC in the combustor unit.

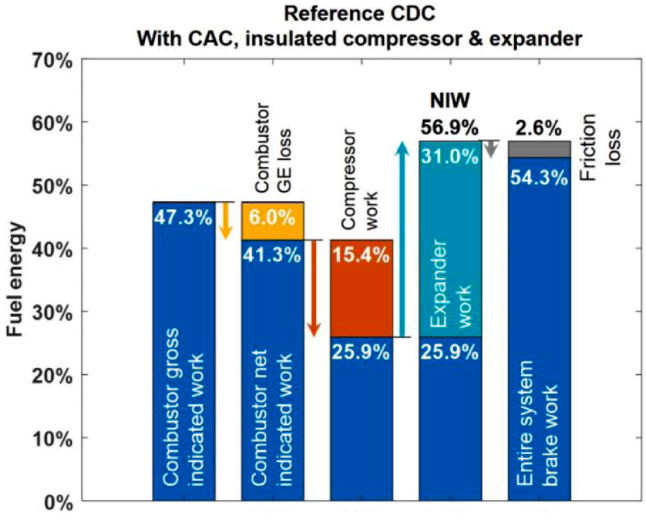

Fig. A3. Engine energy flow from compressor to expander of the DCEE concept using the reference CDC in the combustor with insulated exhaust ports, assuming insulated compressor and expander units and a regular intercooling.

Supplementary materials

Supplementary material associated with this article can be found, in the online version, at doi:10.1016/j.treng.2022.100103.

References

[1] Office of Fossil Energy, HYDROGEN STRATEGY Enabling A Low-Carbon Economy. (2020).
[2] A. Körner, C. Tam, S. Bennett, J. Gagné, Technology Roadmap-Hydrogen and Fuel Cells, Int Energy Agency Paris, Fr, 2015.
[3] J. Baronas, G. Achtelik, et al., Joint Agency Staff Report on Assembly Bill 8: 2019 Annual Assessment of Time and Cost Needed to Attain 100 Hydrogen Refueling Stations in California (2019).
[4] N. Lam, M. Tuner, P. Tunestal, A. Andersson, S. Lundgren, B. Johansson, Double compression expansion engine concepts: a path to high efficiency, SAE Int J Engines 8 (2015) 1562–1578.
[5] N. Lam, A. Andersson, P. Tunestal, Double Compression Expansion Engine Concepts: efficiency Analysis over a Load Range, SAE Technical Paper; (2018).
[6] N. Lam, P. Tunestal, A. Andersson, Simulation of System Brake Efficiency in a Double Compression-Expansion Engine-Concept (DCEE) Based on Experimental Combustion Data, SAE Technical Paper (2019).
[7] V.S.B. Shankar, N. Lam, A. Andersson, B. Johansson, Optimum heat release rates for a double compression expansion (DCEE) engine, SAE Technical Paper (2017).
[8] R. Babayev, A. Andersson, A.S. Dalmau, H.G. Im, B. Johansson, Computational Comparison of the Conventional Diesel and Hydrogen Direct-Injection Compression-Ignition Combustion Engines, Fuel (2021). Submitted.
[9] R. Babayev, A. Andersson, A.S. Dalmau, H.G. Im, B. Johansson, Computational characterization of hydrogen direct injection and nonpremixed combustion in a compression-ignition engine, Int J Hydrogen Energy (2021).
[10] R. Babayev, A. Andersson, A.S. Dalmau, H.G. Im, B. Johansson, Computational Optimization of a Hydrogen Direct-Injection Compression-Ignition Engine for Jet Mixing Dominated Nonpremixed Combustion, Int J Engine Res (2021). Submitted.
[11] https://www.gtisoft.com/gt-suite-applications/propulsion-systems/gt-power-engine-simulation-software/n.d.
[12] G. McTaggart-Cowan, K. Mann, J. Huang, A. Singh, B. Patychuk, Z.X. Zheng, et al., Direct injection of natural gas at up to 600 bar in a pilot-ignited heavy-duty engine, SAE Int J Engines 8 (2015) 981–996.
[13] M.F.M. Zwinkels, S.G. Järås, P.G. Menon, T.A. Griffin, Catalytic materials for high-temperature combustion, Catal Rev Eng 35 (1993) 319–358.
[14] M. Borchers, K. Keller, P. Lott, O. Deutschmann, Selective Catalytic Reduction of NOx with H2 for Cleaning Exhausts of Hydrogen Engines: impact of H2O, O2, and NO/H2 Ratio, Ind Eng Chem Res 60 (2021) 6613–6626.
[15] G. Woschni, A universally applicable equation for the instantaneous heat transfer coefficient in the internal combustion engine, SAE Technical paper (1967).
[16] A.P. Colburn, A method of correlating forced convection heat transfer data and a comparison with fluid friction, Trans Am Inst Chem Engrs 29 (1993) 174–210.
[17] T. Morel, R. Keribar, A model for predicting spatially and time resolved convective heat transfer in bowl-in-piston combustion chambers, SAE Trans (1985) 77–93.
[18] M. Megel, B. Westmoreland, G. Jones, F. Phillips, D. Eberle, M. Tussing, et al., Development of a structurally optimized heavy duty diesel cylinder head design capable of 250 bar peak cylinder pressure operation, SAE Int J Engines 4 (2011) 2736–2755.
[19] D. Crabb, M. Fleiss, J.-.E. Larsson, J. Somhorst, New modular engine platform from Volvo, MTZ Worldw 74 (2013) 4–11.
[20] F.T. Metzner, N. Becker, W. Demmelbauer-Ebner, R. Müller, M.W. Bach, Der neue 6-ı-W12-Motor im Audi A8, MTZ-Motortechnische Zeitschrift 65 (2004) 254–266.
[21] A. Noble, C. Such, Ways to reduce CO2 emissions from on-highway, heavy duty diesel engines, in: Transp. Res. Arena 5th Conf. Transp. Solut. from Res. to DeploymentEuropean Comm. Eur. Dir. Roads Eur. Road Transp. Res. Advis. Counc. WATERBORNETPEuropean Rail Res. Advis. Counc. Inst. Fr. des Sci. Technol. des Transp. l'Aménagement des Réseaux Ministère l'Écologie, du Développement Durable l'Énergie, 2014.
[22] C. Knauder, H. Allmaier, D.E. Sander, T. Sams, Investigations of the friction losses of different engine concepts. part 1: a combined approach for applying subassembly-resolved friction loss analysis on a modern passenger-car diesel engine, Lubricants 7 (2019) 39.
[23] P.K. Senecal, E. Pomraning, K.J. Richards, T.E. Briggs, C.Y. Choi, R.M. McDavid, et al., Multi-dimensional modeling of direct-injection diesel spray liquid length and flame lift-off length using CFD and parallel detailed chemistry, SAE Trans (2003) 1331–1351.
[24] N. Lam, P. Tunestal, A. Andersson, Analyzing Factors Affecting Gross Indicated Efficiency When Inlet Temperature Is Changed, SAE Technical Paper (2018).
[25] H. Kosaka, Y. Wakisaka, Y. Nomura, Y. Hotta, M. Koike, K. Nakakita, et al., Concept of "temperature swing heat insulation" in combustion chamber walls, and appropriate thermo-physical properties for heat insulation coat, SAE Int J Engines 6 (2013) 142–149.
[26] B. Bouteiller, A. Allimant, J.-.M. Zaccardi, J. Cherel, New ceramic thermal barrier coatings development in a spark-ignition engine–experimental investigation, in: International Thermal Spray Conference, ASM International, 2019.
[27] R. Babayev, Isobaric Combustion: a Potential Path to High Efficiency, Combination with the Double Compression Expansion Engine (DCEE) Concept (2018).
[28] R. Babayev, Houidi M Ben, V.S.B. Shankar, B. Aljohani, B Johansson, Injection Strategies for Isobaric Combustion, SAE Technical Paper (2019).
[29] X. Liu, H. Aljabri, B. Mohan, R. Babayev, J. Badra, B. Johansson, et al., A numerical investigation of isobaric combustion strategy in a compression ignition engine, Int J Engine Res n.d. (2022), 1468087420970376.